Monte Carlo Simulations of Grafted Chains at Interfaces

JENNIFER J. SAHLIN, NIKOLAOS A. PEPPAS

Polymer Science and Engineering Laboratories, School of Chemical Engineering, 1283 Chimical Engineering Building (CHME), Purdue University, West Lafayette, Indiana 47907–1283

Received 15 June 1996; accepted 7 September 1996

ABSTRACT: Simulations were carried out of the polymer–polymer chain interpenetration, diffusion, and adhesion of crosslinked polymers with dangling chain ends. Concentration profiles were determined for various polymer chain lengths and densities. The penetration depth was less than the radius of gyration of the polymer grafts or dangling ends and was a function of the packing density and the graft segment length. Limited chain mobility created a stable interfacial zone. © 1997 John Wiley & Sons, Inc. J Appl Polym Sci **64:** 547–551, 1997

Key words: simulations; gel/gel adhesion; chain interpenetration; grafting

INTRODUCTION

A method of significant improvement of polymer/polymer adhesion has been discussed and analyzed in recent years. It refers to the use of short tethered chains, which act as bridges or dangling ends that penetrate across the polymer interface.[1,2] Grafted chains or tethered structures are particularly important in adhesion of polymer networks to other polymers. While the macroscopic adhesive characteristics of polymer networks in contact with other polymers can be evaluated by a variety of experiments, their microscopic behavior is substantially less accessible.[3] The short chain lengths and inhibited bulk motion of these chains dramatically reduce the degree of interdiffusion.[3] As a result, the width of the interfacial region is reduced to such an extent that it may only be measured by techniques such as neutron reflection spectroscopy. Similarly, it is unclear what role chain diffusion plays in the adhesion process of crosslinked polymers.

Thus, the goal of this work was to carry out molecular simulations in order to examine the impact of a variety of variables on the chain interdiffusion of grafted or tethered chains near an interface. As the grafted chains were of uniform molecular size they represented an idealized view of the dangling ends of a crosslinked polymer network[1] or of tethered chains of a compatible polymer on a crosslinked substrate.[4]

Experimentally, the polymers of interest are unique. For example, the desired degree of adhesion for biomedical and drug targeting applications is substantially lower than would be desired for most other applications.[4] As a result, while adhesion of crosslinked polymers has been ignored in the adhesion literature, it is of interest for medical applications. The high swelling ratio typical of most polymer hydrogels also permits much greater molecular mobility than for other crosslinked structures. While the molecular weight of the dangling ends of a polymer network is generally unknown and cannot be systematically controlled by free radical polymerization, the molecular weight of smaller chains that are grafted or tethered onto the gel's surface can be controlled. Thus, the importance of chain interpenetration in crosslinked polymers can be systematically examined by modifying the polymer chain length at the surface of the hydrogel.

Although extensive theoretical work has been

Correspondence to: Nicholas A. Peppas.
Present address: J. J. Sablin, Process Technologies Laboratory, 3M Corporate Research Labs, 3M Center, Building 208-1-01, St. Paul, MN 55101.
Contract grant sponsor: National Institutes of Health.
Contract grant number: GM45027.

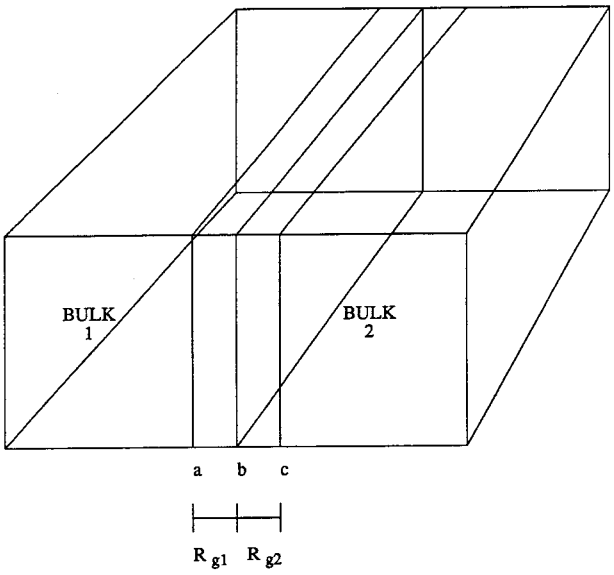

Figure 1 The regions of the initial configuration of the simulation (drawing not to scale). Here, R_{g1} is the radius of gyration for the grafted segments of polymer 1, and R_{g2} is the radius of gyration for the grafted segments of polymer 2.

done to investigate polymer–polymer diffusion in both melts and solution,[5–9] polymer gel systems have not been examined in detail.[10] The simulations discussed in this work are based solely on the entropic effects that may be examined in a lattice system. However, the extent of penetration for grafted chains that are restricted to a lattice is important, because this technique can be used to assess whether diffusion occurs and how the rate of interpenetration is affected by their physically restricted bulk motion. Both the rate of diffusion and the thickness of the interdiffusion zone at specific time intervals can be compared with the results for ungrafted chains. The complexity of the simulation would increase dramatically if enthalpic effects were considered; thus, these simulations model the behavior of a laminate system consisting of two idential polymeric materials.

SIMULATION DESIGN

The dynamic behavior of polymer chains near an interface was studied by performing Monte Carlo molecular simulations on a 40 × 40 × 30 face-centered cubic lattice. A site on this lattice had 12 nearest neighbors with a constant bond length between sites of $a/\sqrt{2}$, where a is the length of the unit cell. This lattice constrains the bond angles of the polymer chains to 0 and 90°. Figure 1 illustrates the initial regions of the lattice.

While moving boundary conditions were maintained in both the x and y directions, a fixed boundary was used in the z direction. Although polymer grafts could diffuse away from the interface and into the bulk polymer, the fixed boundary prevented the subsequent diffusion of polymer chains into the bulk region of the second polymer species without passing across the interface. In the simulation, this back-diffusion problem was avoided by preventing the chains from stepping directly from the (x,y,1) plane to the (x,y,30) plane. Moving boundaries in the other coordinate directions eliminated edge effects. Thus, a smaller lattice was used without affecting the results.

The initial configuration and subsequent chain motions were controlled by specific selection rules. First, the number of monomer units and the density of chains for the grafted chains of polymer 1 and polymer 2 were specified. Subsequently, the fixed chain ends of polymer 1 were randomly positioned in the x, y plane, a, at a distance of one radius of gyration from the interface b. Likewise, the fixed ends of polymer 2 were restricted in a similar manner in plane c. As each chain end was positioned, the chain was randomly grown to its full length before the next polymer's fixed end was positioned. A randomly selected nearest-neighbor site was checked; if it was unoccupied, it was filled by the growing chain. A nearest-neighbor site of this newly occupied position was then selected, and the process was continued. The midpoint of the lattice in the z direction was used as a boundary between the two polymer types. When the appropriate chain density of the first polymer had been obtained, the chains of the second polymer were positioned. All chains were required to be at least 95% of the desired chain length. The region to the left of plane a and to the right of plane c were then randomly filled to the specified bulk density for polymers 1 and 2, respectively.

After the initial configuration was determined, the boundary between the two polymer regions was removed, and the chains were allowed to diffuse across the interface. In the case of oligomers, where each lattice site represented a single atom, the movement of an atom in one chain was restricted by its neighboring atoms. Thus, an atom could only move to a vacant site that was a nearest neighbor to both the previous and next atoms in the chain; the bond length restriction was never violated. This restricted chain motion is illustrated in Figure 2.

During each time increment, the number of randomly selected sites checked was equal to the number of sites in the lattice. If a selected site

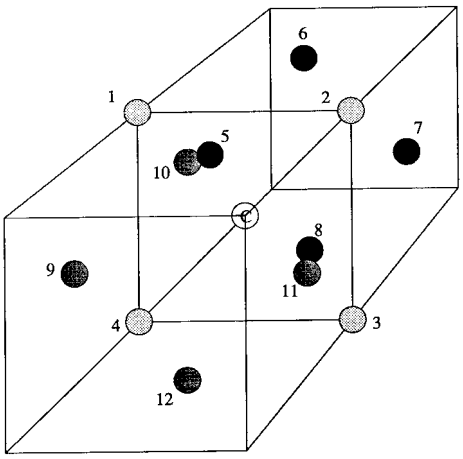

Figure 2 A face-centered cubic lattice. The central atom with four atoms in the central planes 1–4, four atoms in the back planes 5–8, and four atoms in the front planes 9–12.

was empty, a new site was selected. If the site was occupied, one of its nearest neighbor sites was randomly checked. If this new site was open and could be reached without violating the bond length restrictions, then the atom was moved; otherwise, an entirely new site was selected and the procedure continued.

When an atom moved to a new site, the old position was reset to indicate that it was now vacant. Furthermore, the relative position of the two atoms bonded to the atom that had been moved were updated, and the relative position of the atom that was moved was redetermined for the two neighboring atoms. In this manner, the simulation simply keeps track of the type of atom, the relative position of the atoms to which the selected atom is bonded, and whether the selected atom has been previously checked during the present time increment. This technique minimizes the amount of computer memory required, and also conserves the number, size, and type of polymer grafts in the simulation.

The concentration of each type of polymer was subsequently determined as a function of position in the z direction and as a function of time. After a specified number of time increments, the original lattice configuration was reintroduced, and the time steps were repeated. In this manner, the concentration profiles from multiple runs for a set amount of time could be co-added, increasing the effective number of chains in the simulation, and thus reducing the noise in the results.

Simulation results were obtained for oligomer chain lengths of 300, 500, 700, 1000, and 2000 atoms. The density of filled sites was varied from 0.3 to 0.7; both symmetric and asymmetric cases with respect to the chain length and the packing density were investigated. A standard time increment of 1000 was used and the time incrementing process was repeated 10 times for each initial configuration. Thus, a total of 4.8×10^8 sites were checked during a typical simulation. Selected cases were run for 2000 time increments to ascertain that an equilibrium state had been attained in 1000 time steps. Furthermore, several trials were also performed in which the oligomer chains were not permanently fixed to the bulk polymer matrix. In these free-chain cases, the movement of the two chain ends were dictated by the same restrictions.

SIMULATION RESULTS

Figures 3 through 5 are representative results from these simulations. These figures show the normalized concentration of polymer 1 chains as a function of the lattice z-coordinate. The dashed vertical lines indicate the boundary between the bulk and surface regions for the two polymer species. These boundaries are at a distance R_g away from the interface, which is equidistant between lattice z-coordinate 15 and 16. The distance R_g is defined as in Figure 1. In all of these plots, the concentration profile is shown at five time intervals of 0, 250, 500, 750, and 1000. At time 0, the concentration profile is a step function and the slight inclination that is evident in these plots is due to the scaling of the abscissa.

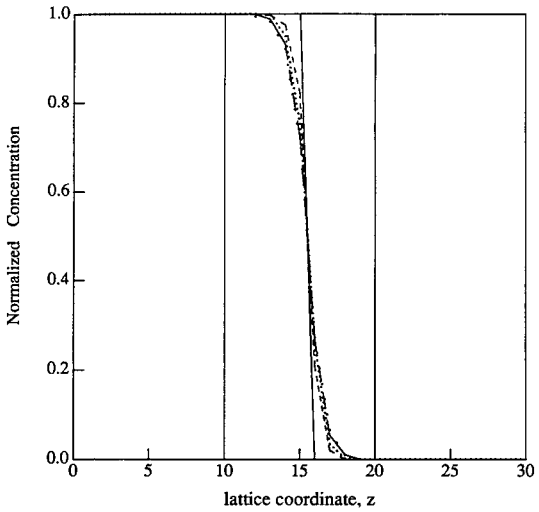

Figure 3 Simulation results of the normalized concentration of grafted polymer chains as a function of axial position: $n_1 = 300$; $n_2 = 300$; $\rho_1 = 0.5$; $\rho_2 = 0.5$.

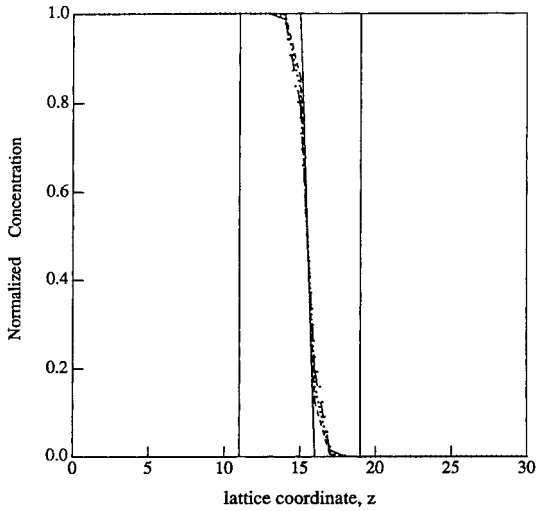

Figure 4 Simulation results of the normalized concentration of grafted polymer chains as a function of axial position: $n_1 = 200$; $n_2 = 200$; $\rho_1 = 0.7$; $\rho_2 = 0.7$.

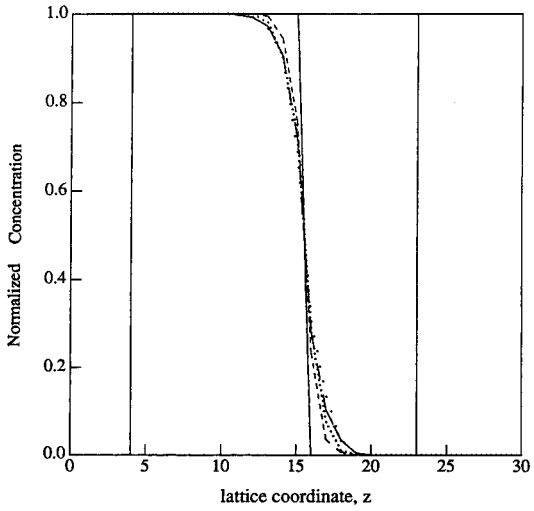

Figure 6 Simulation results of the normalized concentration of grafted polymer chains as a function of axial position: $n_1 = 1500$; $n_2 = 700$; $\rho_1 = 0.3$; $\rho_2 = 0.3$.

Figure 3 shows the concentration profiles for a symmetric system in which the polymer density and the graft lengths are 0.5 and 300, respectively. In this plot, it is evident that diffusion of polymer chains occurs at the interface. However, the depth of penetration is less than the radius of gyration for the polymer grafts.

In Figure 4, the graft segment length has been reduced to 200, while the packing density has been increased to 0.7. This high packing density is not representative of hydrogels, but when these results are compared with those shown in Figure 5, several interesting trends may be noted. In Figure 5, the chain lengths are unchanged, but the packing density has been reduced to 0.3. The concentration profile, which was very steep for ρ_i, is significantly less abrupt when $\rho_i = 0.3$. The graft segments do not, however, diffuse further than R_g.

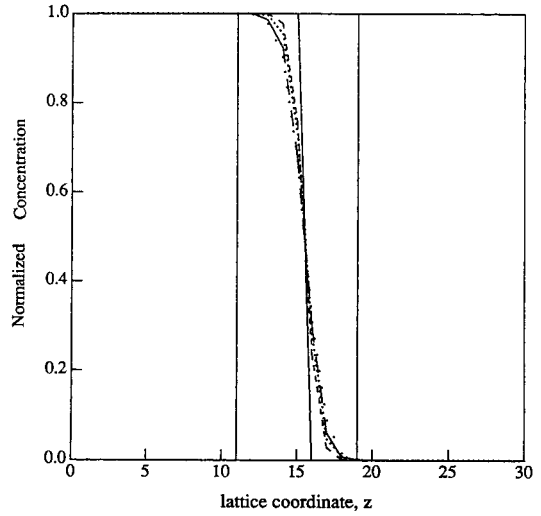

Figure 5 Simulation results of the normalized concentration of grafted polymer chains as a function of axial position: $n_1 = 200$; $n_2 = 200$; $\rho_1 = 0.3$; $\rho_2 = 0.3$.

The penetration depth initially increases with the length of the grafted segments. When the chains are 700 segments long, the interfacial zone does not expand further for simulations performed with a constant chain density of 0.3.

Figure 6 illustrates the effect of an asymmetric system in which polymer 1 grafts contain $n_1 = 1500$ atoms while polymer 2 grafts contain only $n_2 = 700$ atoms. A constant density of 0.3 was used during this simulation. This result shows that the longer chains diffuse slightly further than the shorter segments. However, the interface appears symmetric.

When both the packing density and the graft lengths of the two polymers are different, the interface is no longer symmetric. This is illustrated in Figure 7. Polymer 1, which has a shorter graft length and is diffusing into less dense polymer 2, diffuses further across the interface. Polymer 2 cannot diffuse into polymer 1 as easily, because that polymer is more dense. Thus, the polymer density has a greater impact on the extent of interdiffusion than the graft segment length.

The grafted polymer segments have much lower mobility than polymers of equivalent length that are not bound to the polymer network. Figure 8 illustrates the effect of free polymer chains. Both the packing density and the polymer chain lengths are identical to those given in Figure 7.

In this case, however, the fixed end of the polymer segments has been allowed to move. When this mobility restriction is removed, the interpenetration zone increases from 9 to 13 in the z-coordinate direction. Furthermore, the concentration gradient at the interface is reduced more quickly when the entire polymer chain is free to move. Similar results were obtained for different chain lengths and packing densities.

CONCLUSIONS

These simulations show that polymer chain interdiffusion does occur even for low mobility polymer segments such as polymer grafts. The thickness of the interpenetration zone increases when the chains are not bound to the bulk polymer. However, the concentration gradients persist even at long times. This indicates that although chain mobility is extremely low, segmental diffusion readily occurs. This implies that the adhesive bond strength attained via chain interdiffusion is achieved at relatively short times with respect to the time required to eliminate the concentration gradient.

The difference in the polymer density has a strong effect on the depth of penetration. More void volume is available for diffusion when the matrix density decreases. Increasing the chain length also increases the interpenetration, but the enhancement is not substantial. This simulation clearly shows that the limited polymer mobility creates a stable interfacial zone; the diffusion of entire polymer chains does not occur. The effect of crosslinking and surface-grafting on the fracture energy both support these conclusions. The interpenetration zone was larger for the free chain cases.

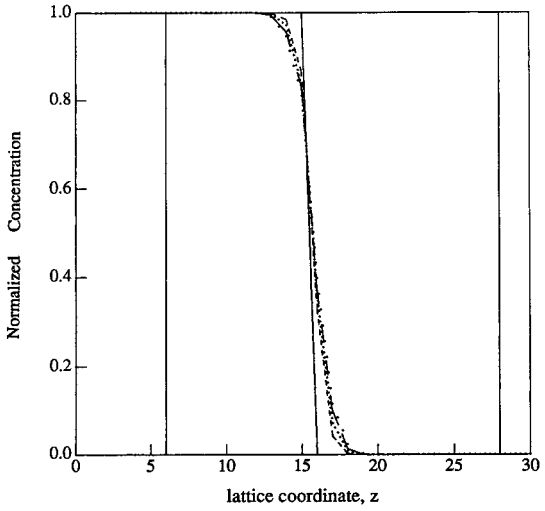

Figure 7 Simulation results of the normalized concentration of grafted polymer chains as a function of axial position: $n_1 = 1000$; $n_2 = 2000$; $\rho_1 = 0.5$; $\rho_2 = 0.3$.

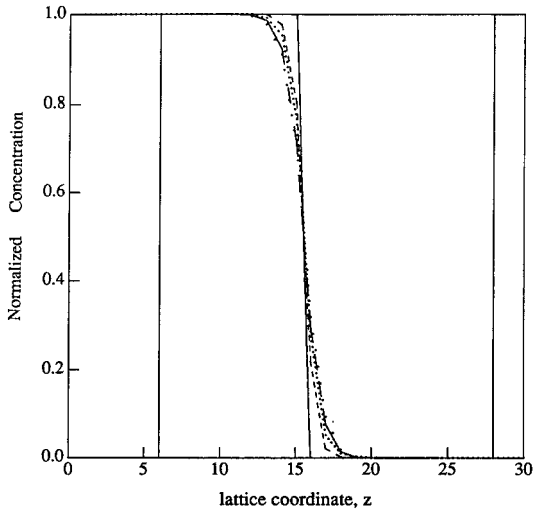

Figure 8 Simulation results of the normalized concentration of free polymer chains as a function of axial position: $n_1 = 1000$; $n_2 = 2000$; $\rho_1 = 0.5$; $\rho_2 = 0.3$.

This work was supported by Grant No. GM 45027 from the National Institutes of Health.

REFERENCES

1. C. Ligoure, *Macromolecules,* **29,** 5459–5468 (1996).
2. H. R. Brown, *IBM J. Res. Dev.,* **38,** 379–390 (1994).
3. A. G. Mikos and N. A. Peppas, *J. Mater. Sci. Lett.,* **8,** 833–834 (1989).
4. J. J. Sahlin and N. A. Peppas, *Biomaterials,* **17,** 1553–1561 (1996).
5. E. J. Kramer, P. Green, and C. J. Palmstrolm, *Polymer,* **25,** 473–480 (1984).
6. J. Reiter, *J. Chem. Phys.,* **94,** 3222–3228 (1991).
7. H. P. Deutsch and K. Binder, *J. Chem. Phys.,* **94,** 2294–2304 (1991).
8. W. Jilge, I. Carmesin, K. Kremer, and K. Binder, *Macromolecules,* **23,** 5001–5013 (1990).
9. M. K. Granfeldt, S. J. Miklavic, S. Marc–Lhelja, and C. E. Woodward, *Macromolecules,* **23,** 4760–4768 (1990).
10. N. A. Rotstein and T. P. Lodge, *Macromolecules,* **25,** 1316–1325 (1992).